

# AquaSAXS: a web server for computation and fitting of SAXS profiles with non-uniformly hydrated atomic models

Frédéric Poitevin<sup>1</sup>, Henri Orland<sup>2</sup>, Sebastian Doniach<sup>3</sup>, Patrice Koehl<sup>4</sup> and Marc Delarue<sup>1,\*</sup>

<sup>1</sup>Institut Pasteur, Unit of Structural Dynamics of Macromolecules, CNRS, URA 2185, <sup>2</sup>Institut de Physique Théorique, CEA-Saclay, 91191 Gif/Yvette Cedex, France, <sup>3</sup>Departments of Physics and Applied Physics and Biophysics Program, Geballe Laboratory of Advanced Materials, Stanford University, Stanford, CA 94305, and <sup>4</sup>Department of Computer Science and Genome Center, University of California, Davis, CA 95616, USA

Received February 18, 2011; Revised May 2, 2011; Accepted May 12, 2011

## ABSTRACT

**Small Angle X-ray Scattering (SAXS) techniques are becoming more and more useful for structural biologists and biochemists, thanks to better access to dedicated synchrotron beamlines, better detectors and the relative easiness of sample preparation. The ability to compute the theoretical SAXS profile of a given structural model, and to compare this profile with the measured scattering intensity, yields crucial structural informations about the macromolecule under study and/or its complexes in solution. An important contribution to the profile, besides the macromolecule itself and its solvent-excluded volume, is the excess density due to the hydration layer. AquaSAXS takes advantage of recently developed methods, such as AquaSol, that give the equilibrium solvent density map around macromolecules, to compute an accurate SAXS/WAXS profile of a given structure and to compare it to the experimental one. Here, we describe the interface architecture and capabilities of the AquaSAXS web server (<http://lorentz.dynstr.pasteur.fr/aquasaxs.php>).**

## INTRODUCTION

Small Angle X-ray Scattering (SAXS) is a technique that allows the study of the structure and interactions of biological molecules in solution. It can be used to probe proteins, nucleic acids, and their complexes under a variety of conditions, from near physiological to highly denaturing, without the need to crystallize the sample

and without the molecular weight limitations inherent in other methods such as NMR spectroscopy.

The increasing availability of high-flux, third-generation synchrotron sources, improvements in detector technology and algorithmic developments for data analysis have made SAXS a technique of choice for a range of biological applications (1).

The basic principle of SAXS is to scatter X-ray photons elastically off molecules in solution, and to record the scattering intensity as a function of the scattering angle. The intensity profile of the buffer is subtracted from the profile of the macromolecule in the buffer, yielding an excess intensity profile, related to the excess electronic density of the molecule and its environment.

The SAXS profile provides information about the global structure and conformation of the studied molecule(s). Several reviews on the physical principles and theory of SAXS describe in detail how the scattering data can be analyzed and how different parameters can be fit and interpreted (2–6). Recent developments and novel applications of SAXS are described in (7–9).

Existing computational approaches for modeling a macromolecular structure based on its SAXS profile can be separated into two classes: profile-to-model (*ab initio* methods) and model-to-profile approaches. The former aims at proposing coarse shapes represented by dummy beads that fit the experimental profile (10–16), while the latter aims at comparing the theoretical profile of a given atomic or coarse grained model to the experimental one (17,18).

The model-to-profile approach consists in computing the theoretical profile of a given atomic structure and providing a measure of the goodness-of-fit to the experimental profile. Here, we describe a web server

\*To whom correspondence should be addressed. Email: [fpoitevi@pasteur.fr](mailto:fpoitevi@pasteur.fr)  
Correspondence may also be addressed to Marc Delarue. Tel: +33 145688605; fax: +33 140613793; Email: [marc.delarue@pasteur.fr](mailto:marc.delarue@pasteur.fr)

(AquaSAXS) that performs this task. It is useful for many applications where one needs to decide whether the proposed model is in agreement with the experiment, and to make assumptions about why they differ, if they do.

Several tools have been designed for that purpose, following various methods (19–24). To our knowledge, the most accurate method to date for computing SAXS profiles of a given macromolecule has been achieved by treating the solvent (excluded and hydrating) explicitly (24). Through this method, even higher resolution profiles resulting from Wide Angle X-Ray Scattering (WAXS) experiments were also reasonably reproduced. However, this approach requires hours of computation to retrieve one profile. All other methods rely on a continuum representation of the solvent-excluded volume, first proposed by Fraser *et al.* (25): the effective-atomic-scattering-form-factor method. The programs SASSIM (22) and Fast-SAXS (23) rely on configurational averaging over Molecular Dynamics simulations to treat the excess in electron density of the hydration layer relative to bulk solvent. The widely used program CRY SOL (19) makes the assumption that the hydration shell surrounding the solute is a constant density layer of given thickness, while FoXS (20) attributes an additional term to every effective-atomic-scattering-form-factor proportional to their solvent accessible area to account for the hydration layer's contribution.

AquaSAXS aims at providing a new way to treat the solvation layer accurately without the need for extensive Molecular Dynamics simulations. To achieve this goal, AquaSAXS takes advantage of recently developed methods that compute the solvent-distribution around a given solute on a 3D grid such as the Poisson–Boltzmann–Langevin (PBL) formalism (26); PBL is implemented in AquaSol that is freely available online as a web server (27) or as a software available upon request from the authors (28). Here it will be run by default. In principle, AquaSAXS can also take advantage of other methods that compute the solvent-distribution surrounding a macromolecule. For example, outputs from 3D-RISM (Three Dimensional-Reference Interaction Site Model) calculations can readily be used by AquaSAXS. The 3D-RISM theory has been implemented in the latest AmberTools package (29).

In addition, AquaSAXS provides a way for the user to check and/or tune the atomic types and the corresponding parameters that are used for computing the solute and the solvent-excluded-volume contribution to the SAXS profile. In the following sections, we describe the method and interface of AquaSAXS.

## AQUASAXS METHOD

In the infinite dilution limit, assuming that the macromolecule has one preferential conformation, the scattering intensity of a sample solution containing the macromolecule is proportional to the scattering intensity of a single macromolecule of scattering density  $\rho_{\text{solute}}(\mathbf{r})$ , surrounded by a solvent of average electron density  $\rho_w$ . The scattering

intensity  $\Delta I$  of this macromolecule at a given value of the wavevector norm  $q$  is the spherical average of the scattering intensity on the sphere of radius  $q$  in reciprocal space (Equation 1).

$$\Delta I(\mathbf{q}) = \int d\Omega A(\mathbf{q})A^*(\mathbf{q}) \quad (1)$$

$$A(\mathbf{q}) = F_{\text{solute}}(\mathbf{q}) - \rho_w F_{\text{sev}}(\mathbf{q}) + \rho_w F_{\text{xhs}}(\mathbf{q})$$

where  $A$  is the excess form factor of the system and  $F_{\text{solute}}$ ,  $F_{\text{sev}}$  are respectively the form factor of the solute *in vacuo* and of the solvent-excluded-volume.  $F_{\text{xhs}}$  is the excess form factor of the hydration shell.

We perform the spherical averaging using the cubature formulae (30). Following the effective-atomic-scattering-form-factor method (25), the solute and the solvent-excluded-volume's form factors are computed as a sum over all  $N$  non-Hydrogen atoms of the solute (Equations 2 and 3).

$$F_{\text{solute}}(\mathbf{q}) = \sum_{j=1}^N f_j(q) e^{i\mathbf{q}\cdot\mathbf{r}_j} \quad (2)$$

$$F_{\text{sev}}(\mathbf{q}) = G(q, C_1) \sum_{j=1}^N (V_j \exp(-\pi V_j^{2/3} q^2)) e^{i\mathbf{q}\cdot\mathbf{r}_j} \quad (3)$$

where  $f_j$  is the atomic form factor *in vacuo* (19), computed as a sum of a constant and four gaussians whose parameters depend on the atom type,  $V_j$  is the solvent volume displaced by atom  $j$ .  $G(q, C_1)$  is an overall expansion factor, as defined in (19), with  $C_1$  being the ratio of the adjusted and computed average atomic radii (default value = 1.0).

Programs such as AquaSol (28) [or 3D-RISM/Amber (29)] compute solvent density maps around the solute, based on the physical interactions within the system. The method used in AquaSol is based on the Poisson–Boltzmann formalism, where the solvent is no longer described as a continuum dielectric medium but rather as an assembly of self-orienting dipoles of variable density on a grid. It was shown that the resulting water distribution is in good agreement with experimental data and with the chemical nature of the atoms exposed to the solvent, both at the atomic and residue-level (26). These maps are typically cubic grids of given size and resolution ( $a$ ), where each grid point  $\mathbf{r}$  is associated to a given density value  $\rho_{\text{solvent}}(\mathbf{r})$ . Basically, in such maps, one expects a density of 0 inside the solute, and 1 (in units of bulk density  $\rho_w$ ) in the bulk region of the solvent, i.e. far from the solute. At the boundary between the solute and bulk region, the density is determined by the physico-chemical nature of the environment.

We compute the form factor for the hydration shell as in Equation 4.

$$F_{\text{xhs}}(\mathbf{q}) = C_2 \sum_j^{N_{\text{grid}}} a^3 (\rho_{\text{solvent}}(\mathbf{r}_j) - 1) e^{-i\mathbf{q}\cdot\mathbf{r}_j} \quad (4)$$

The sum runs over all points with nonzero density. In practice, to reduce computation time, grid points with

a density close to 1 (i.e. typically within  $\pm 1.10^{-4}$ ) are removed from the sum. On Urate Oxidase (example mentioned below), allowing a tolerance of  $1.10^{-6}$  slowed down the computation by a factor of three and did not affect the resulting profile: the same fitting parameters were found, and the goodness-of-fit  $\chi$  (cf Equation 6) was similar (1.688 versus 1.691).

Besides the solute and solvent, another possible contributor to the SAXS profile is the ion atmosphere surrounding the solute. AquaSol (28) computes the density maps of free cations and anions, and, in principle, these maps could be used to compute the excess form factors of ions. However, at physiological concentrations (200 mM NaCl) the ratio of the fugacities of ions and water is  $< 0.5\%$ . At this stage, the contribution of ions was not implemented into AquaSAXS, except in the form of explicitly bound and fixed ions. Nevertheless, the presence of free ions can indirectly affect the solvent density in the hydration shell (screening effect), so the user is prompted for the ionic strength of the solution.

Alternatively, the hydration shell's form factor can be computed as in FoXS (20), following Equation 5.

$$F_{\text{xhs}}^{\text{FoXS-like}}(\mathbf{q}) = C_2 \left( \sum_{j=1}^N s_j e^{i\mathbf{q}\cdot\mathbf{r}_j} \right) f_w(q) \quad (5)$$

where  $s_j$  is the fraction of solvent accessible surface of the atom  $j$  (31) and  $f_w$  is the water form factor.  $C_2$  is a scale factor used to adjust the hydration shell's contribution (default value = 1.0).

The computed profile  $\Delta I$  is fitted to a given experimental SAXS profile  $\Delta I_{\text{exp}}$  (with experimental error  $\sigma$ ) by minimizing the goodness-of-fit function  $\chi$  with respect to three adjustable parameters:  $C_1$ ,  $C_2$  and  $C$  (Equation 6).

$$\chi = \sqrt{\frac{1}{N_q} \sum_{i=1}^{N_q} \left( \frac{\Delta I_{\text{exp}}(q_i) - C \cdot \Delta I(q_i, C_1, C_2)}{\sigma(q_i)} \right)^2} \quad (6)$$

$C_1$  and  $C_2$  values are scanned within a given range ( $0.90 \leq C_1 \leq 1.12$ ,  $0.0 \leq C_2 \leq 1.4$  and  $0.0 \leq C \leq 4.0$ ), in steps of 0.0055, 0.014 and 0.04, *resp.*, and for each pair, a linear-least-squares minimization is performed to adjust the scaling constant  $C$ . The pair leading to the minimal  $\chi$  is kept to compute the returned profile.

## PERFORMANCE OF AQUASAXS

AquaSAXS was successfully tested with all PDB (32) structures that have an experimental SAXS profile in the open access BioIsis database (33), and gave results similar to CRY SOL and FoXS. It was also tested on Urate Oxidase (see Figure 2).

The calculation scales linearly with the number of points at which the profile is sampled ( $N_q$ ), as well as with the number of non-Hydrogen atoms of the solute. It scales to the cube of the number of points per grid edge, although this expensive cost is attenuated by a preliminary compressing process discarding all points with an excess density close to zero.

For the *Solvent-map* solvation option, for maps with 65 grid points per edge (about 2 Å grid size), the calculation typically takes from less than a minute to a few minutes for systems of a few thousands atoms to dozens of thousands of atoms (with  $N_q \simeq 60$ ), which is a few times slower than CRY SOL and FoXS. For a WAXS spectrum,  $N_q \simeq 300$ . For the *Surface-Accessible* solvation option, computation is more efficient.

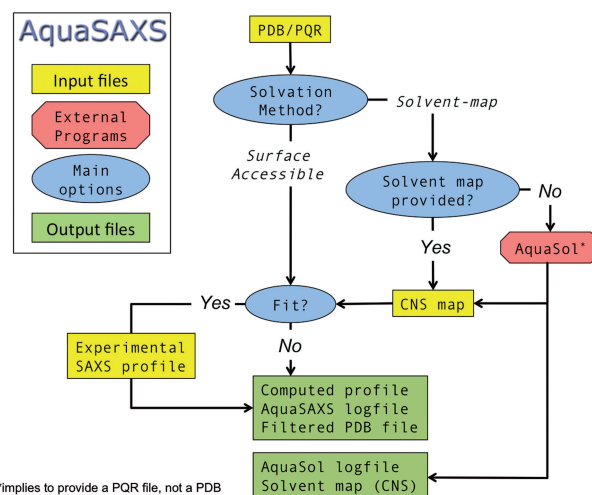
## AQUASAXS WEB SERVER

Figure 1 shows the flowchart of a typical AquaSAXS calculation. Starting with a PDB file or a PQR file, the user is expected to make two decisions, namely the selection of the solvation method, and whether a comparison is made with an experimental SAXS profile or not.

There are three options for the solvation method: either a solvation map is provided as input, or a solvation map is computed using AquaSol (28), or a hydration layer is defined using the accessible surface of each atom, following the method introduced in FoXS (20).

The *Solvent-map* solvation option will account for the hydration layer following Equation 4. If a solvent map (in CNS format) is provided by the user in input, it will be taken into account. If no solvent map is provided, AquaSol (28) will be run in default mode prior to AquaSAXS; in that case, the PDB input file must be in PQR format (34) (partial charges and atomic radius must be known for all atoms). The *Surface-Accessible* solvation option uses a form factor  $F_{\text{xhs}}$  defined as in Equation 5.

Optionally, an ASCII text file containing the experimental SAXS profile can be given as input to AquaSAXS. Lines containing data must consist of at least two columns and an optional, but recommended, third one.



**Figure 1.** Flowchart of AquaSAXS. A PDB or PQR file is mandatory for the calculation, and depending on the chosen method for solvation, a solvent map in CNS format must be fed into the server, or the PDB file must be in PQR format. If one wants to fit a theoretical profile to an experimental one, the latter must be provided as a formatted separate file. After the calculation, the web browser is redirected to the result's page, where the profiles and relative residuals are displayed, as well as a summary of the run. Links toward all output files are provided.

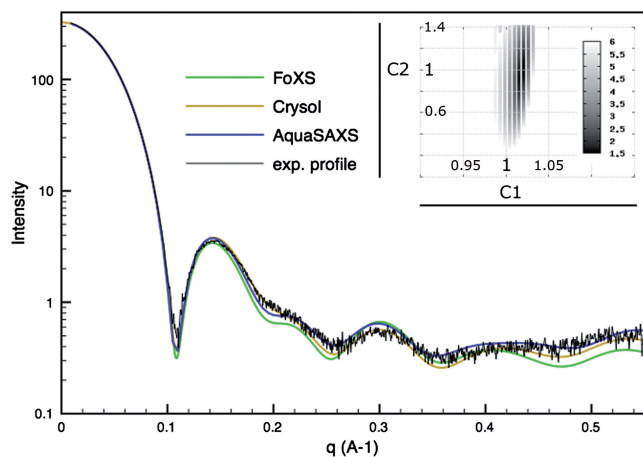


**Figure 2.** Typical result of AquaSAXS on Urate Oxidase. The deposited structure 3L8W was used as model. The PQR file was generated with PDB2PQR (34), using CHARMM parameters. The solvent map was generated with AquaSol. 65 points per edge, equally spaced by 2.2 Å define the cubic grid (using a higher resolution map did not significantly improve the fit). The solute was immersed in an ion atmosphere of 0.1M NaCl, and the solute region was defined by its solvent-accessible surface (with a probe radius of 1.4 Å). One of the profile displayed here (in blue) was output by AquaSAXS after fitting, along with the fitting parameters:  $C_1 = 1.021$  and  $C_2 = 1.022$ . The goodness of fit is:  $\chi = 1.69$ . The computation took less than 5 minutes. 9436 atoms were considered. The profiles fitted using FoXS (green) and CRYSol (orange) are shown for comparison. Their respective values for the goodness-of-fit  $\chi$  is 2.46 and 1.53. FoXS used  $C_1 = 1.09$  and  $C_2 = 2.9$  as fitting parameters, while CRYSol used  $\delta\rho = 0.025$ ,  $R_a = 1.560$  Å and  $\text{Vol} = 179493$  Å<sup>3</sup> (which corresponds to a volume 20% more important than the volume actually deduced from the average radius  $R_a$ ). Additional parameters for CRYSol were the use of up to the 30th order of spherical harmonics, and 18th order for the Fibonacci grid. In every case, the bulk density was set at  $0.334 \text{ e} \cdot \text{Å}^{-3}$ . The figure in inset displays the goodness-of-fit computed by AquaSAXS for the range of  $C_1$  and  $C_2$  scanned by the program. Only values of  $\chi$  between the minimum and 6 are shown, for clarity.

The first column contains the values of the wavevector  $q$ . By default, AquaSAXS defines  $q$  as  $(4\pi s \sin\theta)/\lambda$  in Å<sup>-1</sup>, where  $2\theta$  is the scattering angle and  $\lambda$  is the wavelength of the incident X-ray beam. Three other definitions of  $q$  are also available. The second column contains the scattering intensity values. The optional third column contains the experimental errors. If not provided, the experimental error will be assumed to be equal to the difference between the intensity in  $q_n$ , and the average intensity at  $q_{n-1}$  and  $q_{n+1}$ .

The structure file in PDB or PQR format is mandatory. Each line of the file starting with the label 'ATOM' or 'HETATM' is stored in memory. If the corresponding atom is a hydrogen or belongs to a water molecule, it is discarded. Otherwise, the residue and atom's names are parsed among the standard PDB protein, nucleic acids and ligands library (32). Thirteen atom types are currently recognized: Carbons with zero, one, two or three bound hydrogens, nitrogen with zero, one, two or three bound hydrogens, oxygen with zero or one bound hydrogen, sulfur with zero or one bound hydrogen, and phosphorus. Once the atomic type of atom  $j$  has been recognized, its position  $\mathbf{r}_j$  is stored and it is assigned the corresponding

form factor  $f_j$ , excluded volume  $V_j$  and radius  $r_j$ . On the 'Flowchart' web-page, the user is given the possibility to check whether the atomic types of the residues in the provided PDB/PQR file can be recognized. If the user wants to define other atomic types than those listed above, two optional files can be given as input to the program: one listing the atom types of a given residue, the other listing the atomic parameters of new atom types.

Several other options/parameters can be set: the maximum  $q$ -value considered, the sampling resolution of the profile, the bulk average electron density (in  $\text{e} \cdot \text{Å}^{-3}$ ), the subset chains in the structure to be considered, as well as the values of  $C_1$  and  $C_2$  in the nonfitting mode.

The computation is performed in real time and the browser is redirected to the result's page when the calculation has finished. If an email address is provided, an email will be sent to the user. Depending on the system's size and server's queue load, the typical running time ranges from less than a minute to a few minutes. The result's page displays a plot of the computed profile (see Figure 2), superimposed to the experimental profile, if provided, as well as the run logfile. Links to three output files are displayed, to retrieve the logfile, the profile file, and a PDB file listing all the atoms that have been considered in the calculation. Possibly, links toward the output files of AquaSol (28) are displayed too (computed solvent map and logfile).

## ADDITIONAL FEATURES

In addition to single conformation fitting of experimental SAXS profiles, AquaSAXS provides two methods to deal with multiple structure files.

The first one, called 'Sequential fit', provides a way to compute the SAXS profile of a set of PDB/PQR files in a single run. That way, if an experimental profile is provided, the user can readily compare the relevance of provided models, without having to rerun the server several times.

The second method, called 'Ensemble fit', aims at plugging in all possible models and refining their population, and is directly inspired from (35). This method can prove useful when the macromolecule visits several conformational states in solution. Another interesting way to take profit of this approach would be the following: starting from a given PDB structure, several models are built along a given deformation parameter (e.g. a normal mode); the best value for this deformation parameter would likely be detected by the refinement process.

In practice, this method couples a mean-field optimization of the model's populations with a simulated annealing protocol. Let us consider an ensemble of  $M$  models, each model  $m$  being associated the scattered intensity  $\Delta I_m$ . Noting  $p_m$  the associated probability (or population) of model  $m$ , the total scattered intensity (in the limit of infinite dilution) is then:

$$\Delta I = \sum_{m=1}^M p_m \Delta I_m \quad (7)$$

If one defines a free energy  $F$  of the form:

$$F = \chi - TS$$

$$S = - \sum_{m=1}^M p_m \log p_m \quad (8)$$

where  $\chi$  is defined as in Equation 6,  $S$  is the entropy, and  $T$  is the temperature, then minimizing the free energy with respect to  $p_m$  gives:

$$p_m = (1/Z) \exp(-\beta E_m) \quad (9)$$

where  $\beta$  is the inverse of  $T$ ,  $E_m = \delta\chi/\delta p_m$  and  $Z$  is a normalization constant given by  $1 = \sum_m p_m$ .

The refinement starts with uniform values of the probabilities, which are updated at each cycle of the refinement until a self-consistent solution is obtained; at each cycle the derivative are evaluated at the current solution, i.e. the current set of  $p_m$  values. The temperature governs the contrast between the different populations, the contrast being higher as the temperature is lower. After convergence at a given temperature, the set of populations found is used as initial guess for a new mean-field refinement at lower temperature, until the final temperature is reached.

Results of both methods applied on synthetic data are presented in Supplementary Materials.

## CONCLUSION

We have described a program that allows structural biologists to compare their SAXS data to the theoretical one for a model given as a PDB or PQR file. Its major novelty resides in the possibility to better model the hydration layer through a physically sound representation of the solvent density map, combined with the use of the cubature method for spherical averaging. The user-friendly interface allows to modify (or add new entries to) the list of scatterers and their parameters.

The possibility to fit the data with multiple models, either independently, or through population refinement has also been implemented.

Future developments will allow for the possibility to refine the coordinates of the model against the experimental data. In that case, care must be taken to use as few degrees of freedom as possible. One possibility is to restrict the deformation of the model along a small number of 'essential' normal modes within the framework of the Elastic Network Model (36). Finally, the possibility to compute the theoretical anomalous SAXS profile of a solute containing atoms with anomalous contribution (e.g. Bromide or Cesium ions) will be made available soon.

## SUPPLEMENTARY DATA

Supplementary Data are available at NAR Online.

## ACKNOWLEDGEMENTS

The authors thank Dr Patrice Vachette for kindly providing the Urate Oxidase's experimental SAXS profile and for helpful suggestions on the manuscript. The authors are grateful to Dr Dominique Durand for her help during beta testing, and to Dr Ludovic Sauguet and Dr Hugues Nury for helpful discussions. P.K. acknowledges support from the NIH.

## FUNDING

Funding for open access charge: Institut Pasteur.

*Conflict of interest statement.* None declared.

## REFERENCES

- Grossman, J.G. (2007) Biological solution scattering: recent achievements and future challenges. *J. Appl. Crystallogr.*, **40**, s217–s222.
- Glatter, O. and Kratky, O. (1982) *Small Angle X-ray Scattering*. Academic, London.
- Guinier, A. (1939) La diffraction des rayons X aux très petits angles: application l'étude des phénomènes ultramicroscopiques. *Ann. Phys.*, **12**, 161–237.
- Doniach, S. (2001) Changes in biomolecular conformations seen by small-angle X-ray scattering. *Chem. Rev.*, **101**, 1763–1778.
- Koch, M.H.J., Vachette, P. and Svergun, D.I. (2003) Small-angle scattering: a view on the properties, structures and structural changes of biological macromolecules in solution. *Q. Rev. Biophys.*, **36**, 147–227.
- Svergun, D.I. and Koch, M.H.J. (2003) Small-angle scattering studies of biological macromolecules in solution. *Rep. Prog. Phys.*, **66**, 1735–1782.
- Lipfert, J. and Doniach, S. (2007) Small-angle X-ray scattering from RNA, proteins, and protein complexes. *Annu. Rev. Biophys. Biomol. Struct.*, **36**, 307–327.
- Putnam, C.D., Hammel, M., Hura, G.L. and Tainer, J.A. (2007) X-ray solution scattering (SAXS) combined with crystallography and computation: defining accurate macromolecular structures, conformations and assemblies in solution. *Q. Rev. Biophys.*, **40**, 191–285.
- Rambo, R.P. and Tainer, J.A. (2010) Bridging the solution divide: comprehensive structural analyses of dynamic RNA, DNA and protein assemblies by small-angle X-ray scattering. *Curr. Opin. Struct. Biol.*, **20**, 128–137.
- Chacon, P., Moran, F., Diaz, J.F., Pantos, E. and Andreu, J.M. (1998) Low-resolution structure of proteins in solution retrieved from X-ray scattering with a genetic algorithm. *Biophys. J.*, **74**, 2760–2775.
- Svergun, D.I. (1999) Restoring low-resolution structure of biological macromolecules from solution scattering using simulated annealing. *Biophys. J.*, **76**, 2879–2886.
- Pethoukhov, M.V. and Svergun, D.I. (2003) New methods for domain structure determination of proteins from solution scattering data. *J. Appl. Crystallogr.*, **36**, 540–544.
- Walther, D., Cohen, F.E. and Doniach, S. (2000) Reconstruction of low resolution three-dimensional density maps from one-dimensional small angle X-ray scattering data for biomolecules in solution. *J. Appl. Crystallogr.*, **33**, 350–363.
- Kozin, M.B. and Svergun, D.I. (2001) Automated matching of high- and low-resolution structural models. *J. Appl. Crystallogr.*, **34**, 33–41.
- Volkov, V.V. and Svergun, D.I. (2003) Uniqueness of *ab initio* shape determination in small-angle scattering. *J. Appl. Crystallogr.*, **36**, 860–864.
- Wriggers, W. and Chacon, P. (2001) Using Situs for the registration of protein structures with low-resolution bead

- models from X-ray solution scattering. *J. Appl. Crystallogr.*, **34**, 773–776.
17. Pethoukhov, M.V. and Svergun, D.I. (2005) Global rigid body modeling of macromolecular complexes against small-angle scattering data. *Biophys. J.*, **89**, 1237–1250.
  18. Förster, F., Webb, B., Krukenberg, K.A., Tsuruta, H., Agard, D.A. and Sali, A. (2008) Integration of small-angle X-ray scattering data into structural modeling of proteins and their assemblies. *J. Mol. Biol.*, **382**, 1089–1106.
  19. Svergun, D., Barberato, C. and Koch, M.H.J. (1995) CRY SOL - a program to evaluate X-ray solution scattering of biological macromolecules from atomic coordinates. *J. Appl. Crystallogr.*, **28**, 768–773.
  20. Schneidman-Duhovny, D., Hammel, M. and Sali, A. (2010) FoXS: a web server for rapid computation and fitting of SAXS profiles. *Nucleic Acids Res.*, **38**, W540–W544.
  21. Tjioe, E. and Heller, W.T. (2007) *ORNLSAS*: software for calculation of small-angle scattering intensities of proteins and proteins complexes. *J. Appl. Crystallogr.*, **40**, 782–785.
  22. Merzel, F. and Smith, J.C. (2002) *SASSIM*: a method for calculating small-angle X-ray and neutron scattering and the associated molecular envelope from explicit-atom models of solvated proteins. *Acta Cryst. D*, **58**, 242–249.
  23. Yang, S., Park, S., Makowski, L. and Roux, B. (2009) A rapid coarse residue-based computational method for X-ray solution scattering characterization of protein folds and multiple conformational states of large protein complexes. *Biophys. J.*, **96**, 4449–4463.
  24. Park, S., Bardhan, J.P., Roux, B. and Makowski, L. (2009) Simulated X-ray scattering of protein solutions using explicit-solvent models. *J. Chem. Phys.*, **130**, 134114.
  25. Fraser, R.D.B., MacRae, T.P. and Suzuki, E. (1978) An improved method for calculating the contribution of solvent to the X-ray diffraction pattern of biological molecules. *J. Appl. Crystallogr.*, **11**, 693–694.
  26. Azuara, C., Orland, H., Bon, M., Koehl, P. and Delarue, M. (2008) Incorporating dipolar solvents with variable density in Poisson-Boltzmann electrostatics. *Biophys. J.*, **95**, 5587–5605.
  27. Azuara, C., Lindahl, E., Koehl, P., Orland, H. and Delarue, M. (2006) PDB\_Hydro: incorporating dipolar solvents with variable density in the Poisson-Boltzmann treatment of macromolecule electrostatics. *Nucleic Acids Res.*, **34**, W38–W42.
  28. Koehl, P. and Delarue, M. (2010) AQUASOL: an efficient solver for the dipolar Poisson-Boltzmann-Langevin equation. *J. Chem. Phys.*, **132**, 064101.
  29. Luchko, T., Gusarov, S., Roe, D.R., Simmerling, C., Case, D.A., Tuszynski, J. and Kovalenko, A. (2010) Three-dimensional molecular theory of solvation coupled with molecular dynamics in Amber. *J. Chem. Theo. Comp.*, **6**, 607–624.
  30. Fliege, J. and Maier, U. (1996) A two-stage approach for computing cubature formulae for the sphere. *Technical Report*, Ergebnisberichte Angewandte Mathematik 139T, Universität Dortmund, Fachbereich Mathematik.
  31. Connolly, M.L. (1983) Solvent-accessible surfaces of proteins and nucleic acids. *Science*, **221**, 709–713.
  32. Berman, H., Henrick, K. and Nakamura, H. (2003) Announcing the worldwide Protein Data Bank. *Nat. Struct. Biol.*, **10**, 908.
  33. Hura, G.L., Menon, A.L., Hammel, M., Rambo, R.P., Poole, F.L. 2nd, Tsutakawa, S.E., Jenney, F.E. Jr, Classen, S., Frankel, K.A., Hopkins, R.C. *et al.* (2009) Robust, high-throughput solution structural analyses by small angle X-ray scattering (SAXS). *Nat. Methods*, **6**, 606–612.
  34. Dolinsky, T.J., Nielsen, J.E., McCammon, J.A. and Baker, N.A. (2004) PDB2PQR: an automated pipeline for the setup of Poisson-Boltzmann electrostatics calculations. *Nucleic Acids Res.*, **32**, W665–W667.
  35. Delarue, M. (2008) Dealing with structural variability in molecular replacement and crystallographic refinement through normal-mode analysis. *Acta Cryst.*, D40–D48.
  36. Nicolay, S. and Sanejouand, Y.-H. (2006) Functional modes of proteins are among the most robust. *Phys. Rev. Letter*, **96**, 078104–112.